Journal of Medicinal Chemistry

Article

Cite This: J. Med. Chem. XXXX, XXX, XXX−XXX

pubs.acs.org/jmc

Structure-Based Discovery of CF53 as a Potent and Orally Bioavailable Bromodomain and Extra-Terminal (BET) Bromodomain Inhibitor

Yujun Zhao,[†,⊥,○] Bing Zhou,[†,⊥,○] Longchuan Bai,[†] Liu Liu,[†] Chao-Yie Yang,[†] Jennifer L. Meagher,[‡] Jeanne A. Stuckey,[‡] Donna McEachern,[†] Sally Przybranowski,[†] Mi Wang,[†] Xu Ran,[†,#] Angelo Aguilar,[†] Yang Hu,[†] Jeff W. Kampf,[§] Xiaoqin Li,[∥] Ting Zhao,[∥] Siwei Li,[∥] Bo Wen,[∥] Duxin Sun,[∥] and Shaomeng Wang*[,†]

[†]Rogal Cancer Center and Departments of Internal Medicine, Pharmacology, and Medicinal Chemistry, [‡]Life Sciences Institute and Department of Biological Chemistry, [§]Department of Chemistry, and [∥]Department of Pharmaceutical Sciences, College of Pharmacy, University of Michigan, Ann Arbor, Michigan 48109, United States

Supporting Information

ABSTRACT: We report the structure-based discovery of CF53 (**28**) as a highly potent and orally active inhibitor of bromodomain and extra-terminal (BET) proteins. By the incorporation of a NH-pyrazole group into the 9H-pyrimido[4,5-*b*]indole core, we identified a series of compounds that bind to BRD4 BD1 protein with K_i values of <1 nM and achieve low nanomolar potencies in the cell growth inhibition of leukemia and breast cancer cells. The most-promising compound, CF53, possesses excellent oral pharmacokinetic properties and achieves significant antitumor activity in both triple-negative breast cancer and acute leukemia xenograft models in mice. Determination of the co-crystal structure of CF53 with the BRD4 BD1 protein provides a structural basis for its high binding affinity to BET proteins. CF53 is very selective over non-BET bromodomain-containing proteins. These data establish CF53 as a potent, selective, and orally active BET inhibitor, which warrants further evaluation for advanced preclinical development.

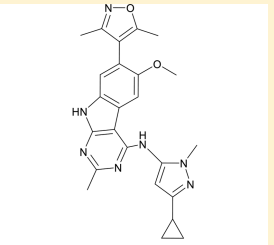

INTRODUCTION

Bromodomain and extra-terminal (BET)-family proteins include BRD2, BRD3, BRD4, and a testis-specific protein, BRDT.[1−4] The N-terminal domain of the BET family proteins contains two tandem and characteristic bromodomains (BRD), BD1 and BD2, which share high sequence homology and structural similarities and are a common feature of BET proteins.[4,5] The BET BRD domains function as recognition motifs for interaction with acetylated lysine residues (AcK) in histone tails and anchor their associated proteins to the target gene promoter and enhancer sites in chromatins.[6−10] BET proteins are thus critical epigenetic "readers" and play a key role in the regulation of gene transcription. They are attractive new therapeutic targets for cancers and a number of other human diseases.[1,2,11]

In recent years, a number of classes of potent and specific small-molecule inhibitors of BET proteins (hereafter called BET inhibitors) have been developed, with representative compounds shown in Figure 1. JQ-1 (**1**) was the first reported potent and specific BET inhibitor[10] and has been extensively employed to evaluate the therapeutic potential of BET inhibitors in a large number of preclinical human disease models. Several BET inhibitors have subsequently advanced into clinical development.[12,13] For examples, compounds **3**,[14,15] **4**,[16] **5**,[17] **6**,[18] and **7**[19,20] are currently being evaluated in phase I and phase II clinical trials for treatment of hematological malignancies and solid tumors, and compound **8**[21,22] has been tested as a new therapy for the treatment of type II diabetes and chronic kidney failure. Recently reported early clinical data for compounds **3**[14,15] and **5**[17] have also provided clinical evidence that small-molecule BET inhibitors may have therapeutic potential for the treatment of several forms of human cancer.

In our ongoing efforts to identify a potent and selective BET inhibitor for clinical development, we recently reported **9** (4-(6-methoxy-2-methyl-4-(quinolin-4-yl)-9H-pyrimido[4,5-*b*]-indol-7-yl)-3,5-dimethylisoxazole; CD161)[23] as a potent and orally bioavailable BET bromodomain inhibitor. Compound **9** binds to BET proteins with low nanomolar affinities and demonstrates high selectivity over 24 non-BET proteins containing bromodomains.[23] It shows potent cell growth inhibitor activity in acute leukemia cell lines harboring mixed lineage leukemia 1 (MLL1) fusion protein and in a panel of human breast cancer cell lines.[23] Compound **9** has a good pharmacokinetic profile in mice and rats and demonstrates strong antitumor activity in MV4;11 acute leukemia and MDA-MB-231 breast cancer xenograft models. Overall, compound **9** is a promising lead compound for further optimization toward the identification of a suitable clinical candidate.

During the course of our investigation, we found that compound **10** (CD235), a structurally similar analogue of **9**,

Received: March 27, 2018

DOI: 10.1021/acs.jmedchem.8b00483
J. Med. Chem. XXXX, XXX, XXX−XXX

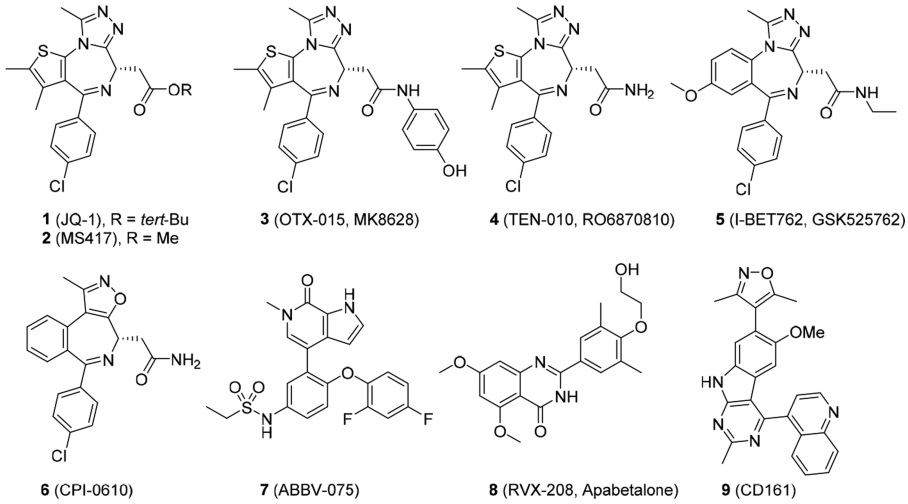

Figure 1. Representative previously reported potent BET bromodomain inhibitors.

shows restricted rotation of the C−C bond that connects the quinoline and 9H-pyrimido[4,5-*b*]indole moieties and has a pair of enantiomers in the single crystal structure (Figure 2),

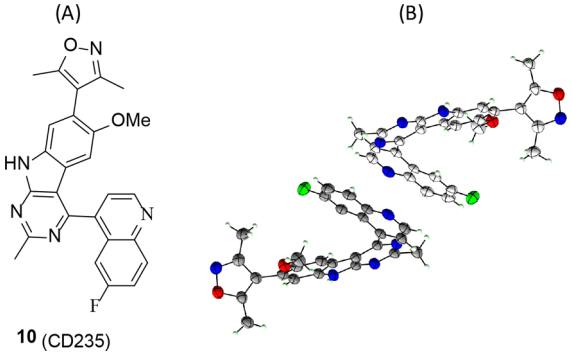

Figure 2. (A) Chemical structure of **10** and (B) single-crystal structure of **10**. The single-crystal structure shows the restricted rotation of the C−C bond that connects the quinoline and 9*H*-pyrimido[4,5-*b*]indole and contains a pair of enantiomers in the crystal unit.

which presents a potential manufacturing challenge for further development for this class of compounds. We decided to perform modifications of compound **9** to remove the rotationally restricted C−C bond.

In the present study, we report the identification of a number of highly potent, orally bioavailable, and achiral small-molecule BET inhibitors. Our effort yielded the discovery of compound **28** (CF53) as a promising BET inhibitor suitable for advanced preclinical development.

RESULTS AND DISCUSSION

Our optimization effort started with removal of the restricted C−C bond that connects the quinoline and 9*H*-pyrimido[4,5-*b*]indolein **9** and **10**. We reasoned that addition of a single nitrogen atom between the 9*H*-pyrimido[4,5-*b*]indole core and the quinoline moiety will generate achiral compounds that can rotate freely. We synthesized compound **12** (Table 1) bearing a1-methyl-1H-indazol-3-amine moiety based on compound **11** (CD134) because **11** has higher binding affinities to BET proteins than those of compound **9**.[23,24] Because BRD4 BD1, but not the BD2 domain, was shown to regulate gene

Table 1. Optimization of 9 with NH-Indazole-Type Substitutions

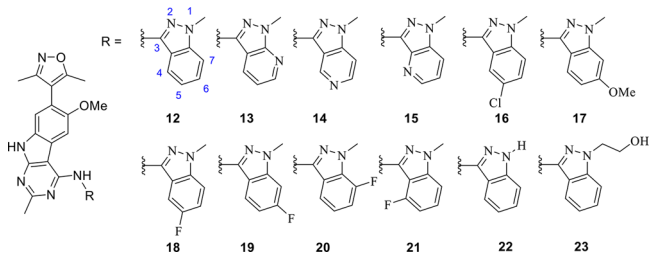

ID	BRD4 BD1	
	IC_{50} (nM)[a]	K_i (nM)
9(CD161)	28.2 ± 4.4	8.2 ± 1.2
11(CD134)	6.1 ± 1.4	0.8 ± 0.1
12	9.1 ± 0.8	0.7 ± 0.3
13	20.8 ± 0.6	4.9 ± 0.2
14	228.1 ± 17.3	77.9 ± 6.0
15	228.5 ± 25.9	78.0 ± 9.0
16	>1000	
17	195.9 ± 6.0	66.5 ± 2.0
18	54.5 ± 1.8	16.7 ± 0.6
19	87.6 ± 3.3	28.4 ± 1.1
20	95.2 ± 8.8	31.0 ± 3.1
21	68.0 ± 2.0	21.5 ± 0.7
22	11.8 ± 0.7	1.7 ± 0.2
23	9.8 ± 0.2	1.0 ± 0.1

[a]Mean of three experiments.

transcription,[25] we first evaluated the binding affinities of **12** and other synthesized compounds first for their binding affinities to the BRD4 BD1 protein for our structure−activity relationship studies.

Compound **12** binds to BRD4 BD1 with a high affinity (IC_{50} = 9.1 nM and K_i = 0.7 nM). Based upon the encouraging binding data for **12**, the subsequent optimization of 1-methyl-1H-indazol-3-amine moiety was carried out, and the results are summarized in Table 1.

Replacement of one carbon atom at the 7 position of **12** by a nitrogen yielded **13**, which binds to BRD4 BD1 with an affinity similar to that of **12**. Incorporation of a nitrogen atom at the 5 or 6 position of **12** led to **14** and **15**, respectively, which have

DOI: 10.1021/acs.jmedchem.8b00483
J. Med. Chem. XXXX, XXX, XXX−XXX

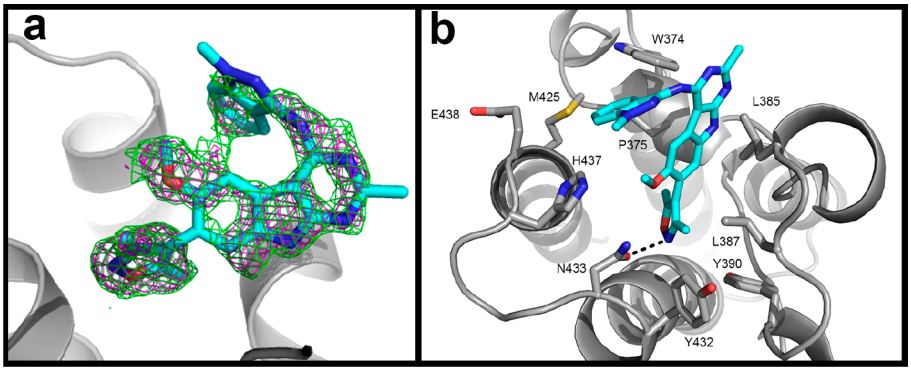

Figure 3. X-ray co-crystal structure of compound **12** in complex with BRD4 BD2 determined at a 1.5 Å resolution (PDB ID: 6C7Q). (a). The Fo−Fc omission electron-density map of **12** contoured at 2σ (magenta) and 1.5σ (green). The protein backbone is shown in gray. (b). Detailed interactions of compound **12** with BRD4 BD2. The protein backbone is shown in gray, with the side chains of residues interacting with compound shown as sticks. Carbon is depicted in cyan, nitrogen in blue, oxygen in red, and sulfur in yellow. Hydrogen bonds are shown as dashed lines.

much weaker binding affinities to BRD4 BD1 than **12**. Substitution of the benzene ring of the 1-methyl-1H-indazole moiety of **12** with a halogen atom or a methoxyl group at different positions yielded compounds **16**−**21**, which failed to improve binding affinities to BRD4 BD1 over that of **12**. Removal of the methyl group from the 1-methyl-1H-indazole moiety or replacing it with 2-hydroxyethyl yielded compounds **22** and **23**, respectively, which bind to BRD4 BD1 with high affinities (K_i values of 1−2 nM).

To facilitate our further optimization effort, we determined the co-crystal structure of **12** complexed with BRD4 BD2 (PDB ID: 6C7Q; Figure 3). A comparison of the co-crystal structures for compounds **9** and **12** complexed with either BRD4 BD1 or BRD4 BD2 shows that the same 3,5-dimethyl isooxazole and 9*H*-pyrimido[4,5-*b*]indole moieties in **9** and **12** have very similar binding modes, while the benzene ring of the NH-indazole group in **12** is inserted into the WPF hydrophobic pocket.

Our co-crystal structure for **12** further shows that while the WPF pocket nicely accommodates the benzene ring of the indazole group in **12**, the pocket could fit a bulkier group for enhanced hydrophobic interactions. We therefore decided to replace the NH-indazole group in **12** with a substituted NH-pyrazole and synthesized a series of compounds (**24**−**40**) whose binding affinities to BRD4 BD1 are summarized in Table 2.

Compound **24**, containing a simple 1,3-dimethyl-1H-pyrazole moiety, binds to BRD4 BD1 with an IC_{50} value of 9.4 nM (K_i = 1.9 nM). Encouraged by the strong binding affinity of **24**, we synthesized **26**, **27**, and **28** by replacing the methyl group at the 3 position of the pyrazole with an isopropyl, a *t*-butyl, or a cyclopropyl group, respectively. These three compounds bind to BRD4 BD1 with K_i values of <1, 1.2, and <1 nM, respectively. Replacing the 3-methyl group in **24** with CF_3 yielded **25**, which is slightly less potent than **24** in its binding to BRD4 BD1.Changing the cyclopropyl group in **28** to cyclobutyl resulted in **29**, which is less potent than **28**. Substituting one of the three methyl groups in the *t*-butyl group of **27** with a CF_3 group generated **30**, which has a high affinity to BRD4 BD1, very similar to that of **27**.

We next investigated the effect of replacing the 1-methyl group of the pyrazole in **24** with other small hydrophobic groups, and produced **31**, **32**, **33**, **34**, and **35**. Compounds **32**, **33**, and **35** have similar binding affinities to BRD4 BD1 to that of **24** but **31** and **34** have higher affinities than **24** for BRD4 BD1.

We synthesized **36** by replacing the 1,3-dimethyl-1H-pyrazole moiety in **24** with 1,5-dimethyl-1H-pyrazole and found that **36** is several times less potent than **24** in binding to BRD4 BD1. We installed a 4-methyl substituent in the 1,3-dimethyl-1H-pyrazole moiety of **24**, which led to **37**. Compound **37** is more than 5 times less potent than **24** in binding to BDR4 BD1.

Table 2. Optimization of 9 with *N*-Pyrazole-Type Substitutions

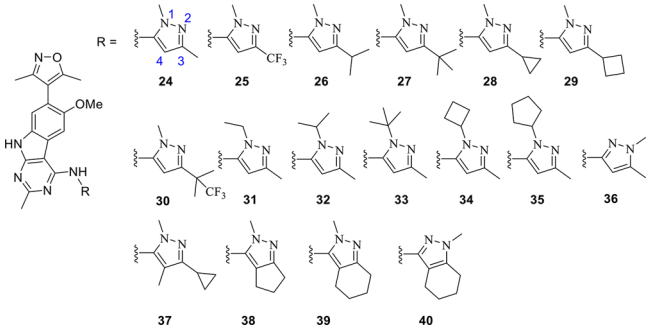

ID	BRD4 BD1	
	IC_{50} (nM)[a]	K_i (nM)
24	9.4 ± 0.6	0.8 ± 0.2
25	15.8 ± 0.4	3.1 ± 0.1
26	6.1 ± 0.1	<1
27	10.5 ± 1.2	1.2 ± 0.4
28 (CF53)	2.0 ± 0.3	<1
29	12.8 ± 2.1	2.0 ± 0.7
30	13.8 ± 0.6	2.4 ± 0.2
31	16.8 ± 2.5	3.4 ± 0.8
32	6.1 ± 0.2	0.5 ± 0.1
33	4.4 ± 0.4	<1
34	14.3 ± 2.5	2.6 ± 0.9
35	4.0 ± 0.2	<1
36	24.9 ± 1.8	6.3 ± 0.6
37	51.7 ± 7.9	15.8 ± 2.8
38	5.5 ± 1.0	<1
39	4.9 ± 0.5	<1
40	5.0 ± 0.3	<1

[a]Mean of three experiments

DOI: 10.1021/acs.jmedchem.8b00483
J. Med. Chem. XXXX, XXX, XXX−XXX

We next synthesized **38** and **39** based on **24** with a fused 5- or 6-membered ring, respectively. Both **38** and **39** bind to BRD4 BD1 with high affinities (K_i< 1 nM) and are more potent than **24**. We synthesized **40** by moving the 1-methyl group in the pyrazole moiety of **39** to the 2 position. Compound **40** has a high affinity to BRD4 BD1, similar to that of **39**. Thus, our further optimization of compound **24** yielded a number of very-high-affinity BRD4 BD1 inhibitors.

We employed the MOLM-13 acute leukemia and MDA-MB-231breast cancer cell lines to evaluate the cell growth inhibitory activity of these BET inhibitors in Table 2. The data obtained are summarized in Table 3.

Table 3. Inhibition by BET Inhibitors of Cell Growth in MOLM-13 andMDA-MB-231 Cell Lines

ID	MOLM-13 IC_{50} (nM)[a]	MDA-MB-231 IC_{50} (nM)[a]	ID	MOLM-13 IC_{50} (nM)[a]	MDA-MB-231 IC_{50} (nM)[a]
24	10.3	55.1	**33**	10.6	13.9
25	56 ± 23	156 ± 13	**34**	38.8	26
26	11.7	26.0	**35**	17.7	25.0
27	23.0	23.5	**36**	30.7	81.1
28	7 ± 3	85 ± 12	**37**	201	319
29	26.6	63.2	**38**	5 ± 1	67 ± 9
30	75	164	**39**	11.3	17.5
31	15.4	26.3	**40**	41.9	58.3
32	5.0	29.6			

[a]Mean of three experiments for compounds **25**, **28**, and **38**

Consistent with its high affinity to BRD4 BD1, **24** potently inhibits cell growth in both the MOLM-13 acute leukemia cell line and the MDA-MB-231 breast cancer cell line with IC_{50} values of 10.3 and 55.1 nM, respectively. Several analogues of **24** also have very potent cellular activity with **28**, **33**, **38**, and **39** being the most-potent compounds in this series of compounds. Compounds **28**, **33**, **38**, and **39** achieve IC_{50} values of 11.7, 10.6, 6.0, and 11.3 nM, respectively, in the MOLM-13 cell line, and 11.2, 13.9, 7.8, and 17.5 nM in the MDA-MB-231 cell line, respectively. In general, compounds with weaker binding affinities than **24** to BRD4 were found to have weaker cellular activity in both cell lines. For example, compounds **30** and **37** have IC_{50} values of 75 and 201 nM in the MOLM-13 cell line and 164 and 319 nM in the MDA-MB-231 cell line, respectively.

We next assessed the exposure of 6 representative potent BET inhibitors in plasma and in the xenograft tumor tissue in tumor-bearing mice with 2 time points upon administration for each compound (Table 4). Our data showed that these BET inhibitors all have good oral exposure in the plasma, with **28** being the best. Additionally, several compounds, including **28**, **33**, and **38**, achieve good drug exposure in the tumor tissue (again, with **28** being the best).

Based on the initial oral exposure data, **28** was identified as an orally bioavailable, promising BET inhibitor. We next determined the pharmacokinetics of **28** in mice, with the data summarized in Table 5. Compound **28** achieves a cMax of 6.4 μM and an AUC of 32.2 μM/hr with 25 mg/kg oral administration and has an oral bioavailability (F, %) of 71.3%. Compound **28** (CF53) has a reasonable aqueous solubility of 19.5 ± 5.5, 72.6 ± 1.3, and 14 ± 0.5 μM at pH of 3, 7.4, and 11, respectively.

To gain structural insights into the high binding affinity of **28** to BRD4 BD1 protein, we determined a high-resolution co-

Table 4. Oral Exposure in Plasma and Tumor Tissues of Six Potent BET Inhibitors in Mice[a]

ID	plasma concentration (ng/mL)[b] (time point)	tumor concentration (ng/g)[b] (time point)
26	6245 (1 h)	736 (1 h)
	1874 (6 h)	166 (6 h)
27	923 (1 h)	305 (1 h)
	458 (6 h)	268 (6 h)
28(CF53)	12600 (1 h)	7375 (1 h)
	7365 (6 h)	3671 (6 h)
33	3675 (0.5 h)	5231 (0.5 h)
	127 (6 h)	621 (6 h)
38	4880 (1 h)	1509 (1 h)
	1584 (6 h)	600 (6 h)
39	2983 (1 h)	466 (1 h)
	1150 (6 h)	132 (6 h)

[a]Each compound was administered at 50 mg/kg via oral gavage. [b]Mean of drug concentrations obtained from two mice per tumor for each time-point.

Table 5. Pharmacokinetic Parameters of 28 (CF53) in Mice

	route/ dose	$T_{1/2}$ (h)	Cmax (μg/ mL)	AUC (μM × h)	Cl (L/h/kg)	Vz (L/kg)	F (%)
28	IV/5 mg/kg	–	–	9.05	1.25	0.83	–
	PO/25 mg/kg	1.0	6.40	32.2	–	–	71.3

crystal structure at 1.5 Å resolution of **28** in a complex with BRD4 BD1 (Figure 4, PDB ID: 6C7R). The co-crystal structure shows that the 3,5-dimethylisooxazole has an H-bond interaction with the conserved water molecules inside the pocket. The 9*H*-pyrimido[4,5-*b*]indole moiety of **28** has a binding model similar to that of **9** and **12**. The pyrazole projects its 3-cyclopropyl group into the hydrophobic WPF pocket. This high-resolution co-crystal structure thus shows that **28** has optimal interactions with BRD4 BD1, providing a structural basis for the high-affinity binding.

We evaluated the binding affinities of **28** to the family of BET proteins and its selectivity over bromodomain-containing proteins in the BROMOscan assays by DiscoverX,[26] and the results are summarized in Table 6. The data showed that **28** binds to both the BD1 and BD2 domains of BRD2, BRD3, BRD4, and BRDT BET proteins with high affinities (K_d = 0.49−2.2 nM). Beyond the BET family proteins, **28** displays good affinities to CREBBP, CRCR2, and EP300 with K_d values of 47, 571, and 110 nM, respectively, but shows no appreciable binding affinity to 23 other non-BET family bromodomain containing proteins at concentrations of 3−4 μM. Hence, compound **28** shows >50-fold selectivity for BET bromodomains over CRCR2 and EP300 and >20-fold over CREBBP. We also evaluated the inhibition of CF53 against a panel of 372 kinases by Reaction Biology (Malvern, PA). The kinase activity data showed that CF53 has an IC_{50} value of 3.9 μM against PLK4 and has no appreciable inhibition against other 371 kinases at 3 μM. Hence, **28** is a very potent BET inhibitor and demonstrates a high selectivity over the other bromodomain-containing proteins and kinases.

We evaluated **28** for its in vivo efficacy in the MDA-MB-231 triple-negative breast cancer and RS4;11 acute leukemia xenograft models in mice, with **3** (OTX015) included as the control compound (Figures 5 and 6) because OTX015 has

DOI: 10.1021/acs.jmedchem.8b00483
J. Med. Chem. XXXX, XXX, XXX−XXX

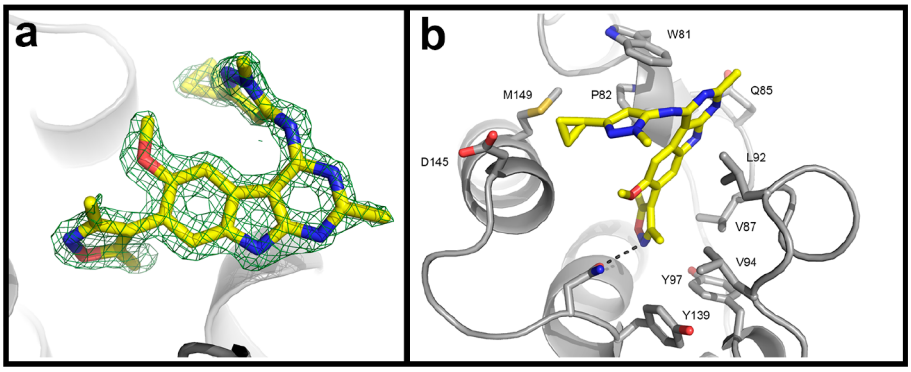

Figure 4. X-ray co-crystal structure of compound **28** (CF53) in complex with BRD4 BD1 protein determined at a 1.5 Å resolution (PDB ID: 6C7R). (a) The Fo−Fc omission electron-density map of CF53 contoured at 3σ. Protein backbone is shown in gray cartoon. (b) Detailed interactions of compound **28** with BRD4 BD1. The protein backbone is shown in gray, with the side chains of residues interacting with the compound shown as sticks. For **28**, carbon is depicted in yellow, nitrogen in blue, oxygen in red, and sulfur in yellow. Hydrogen bonds are shown as dashed lines.

Table 6. Binding Affinities of 28 (CF53) to Different BET Proteins and Selectivity over Other Bromodomain-Containing Proteins, Measured with the DiscoverX BROMO Scan Platform[26]

protein	K_d (nM)	protein	K_d (nM)	protein	K_d (nM)
BRD2 (BD1)	1.1	CREBBP	47	BRPF3	>5000
BRD2 (BD2)	0.6	CECR2	570	FALZ	>5000
BRD3 (BD1)	0.52	EP300	110	GCN5L2	>5000
BRD3 (BD2)	0.49	ATAD2A	>5000	PBRM1(2)	>3000
BRD4 (BD1)	2.2	ATAD2B	>5000	PBRM1(5)	>5000
BRD4 (BD2)	0.8	BAZ2A	>5000	PCAF	>5000
BRDT (BD1)	2	BAZ2B	>5000	SMARCA2	>5000
BRDT (BD2)	2.1	BRD1	>5000	SMARCA4	>5000
		BRD7	>5000	TAF1L (BD2)	>5000
		BRD8 (BD1)	>5000	TAF1 (BD2)	>5000
		BRD8 (BD2)	>5000	TRIM24	>4000
		BRD9	>5000	TRIM33 (PHD, Bromo)	>5000
		BRPF1	>4000	WDR9 (BD2)	>5000

been advanced into phase II clinical trials for the treatment of human cancer. At 25 and 50 mg/kg, compound **28** was found to be effective in the inhibition of tumor growth in both models. In the MDA-MB-231 xenograft tumor model, **28** achieves tumor growth inhibition (TGI) of 67.6% and 77.3% with 25 and 50 mg/kg doses at the end of treatment (day 44) as compared to the control treatment with a p value of <0.001 for both doses. In comparison, **3** (OTX015) shows only 21.0% TGI at 50 mg/kg (p = 0.056) in the MDA-MB-231 xenograft model at the end of the treatment (day 44). In the RS4;11 model, **28** achieves TGI of 49.3% and 72.3% with 25 and 50 mg/kg doses at the end of treatment (day 35) as compared to the control treatment with a p value of <0.005 for both doses. In comparison, **3** (OTX015) at 50 mg/kg shows a TGI of 33.0% at 50 mg/kg (p = 0.036) in the RS4;11 xenograft model at the end of the treatment (day 35). Significantly, **28** induces no more than 5% of weight loss or does not cause other signs of toxicity in mice at all 3 of the dose schedules tested. Our efficacy data showed that **28** (CF53) is effective in inhibition of tumor growth in the MDA-MB-231 triple-negative breast cancer and RS4;11 acute leukemia models at well tolerated-dose schedules and is more effective than **3** (OTX015), a BET inhibitor currently in clinical development.

CHEMISTRY

Compounds **12**−**40** were synthesized from 4-(4-chloro-6-methoxy-2-methyl-9H-pyrimido[4,5-*b*]indol-7-yl)-3,5-dimethylisoxazole (S13) and the corresponding 3-amino-1*H*-

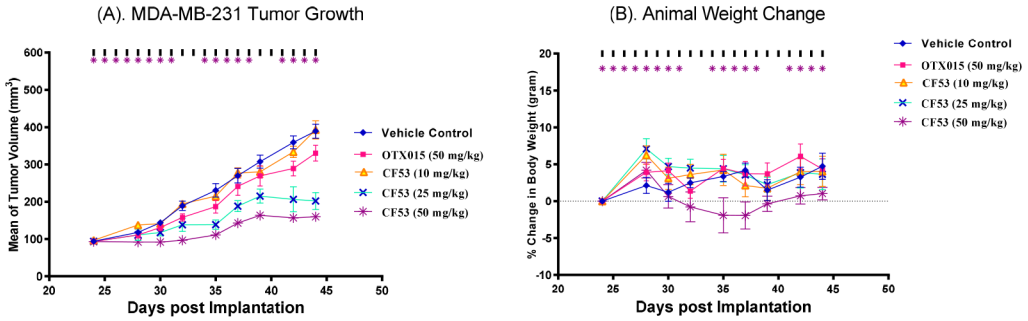

Figure 5. Antitumor efficacy of **28** (CF53) and **3** (OTX015) in the MDA-MB-231 xenograft model in severe combined immunodeficient (SCID) mice. These compounds were administered via oral gavage at indicated dose schedules. (A) Tumor growth inhibition. (B) Percentage of animal weight change.

DOI: 10.1021/acs.jmedchem.8b00483
J. Med. Chem. XXXX, XXX, XXX−XXX

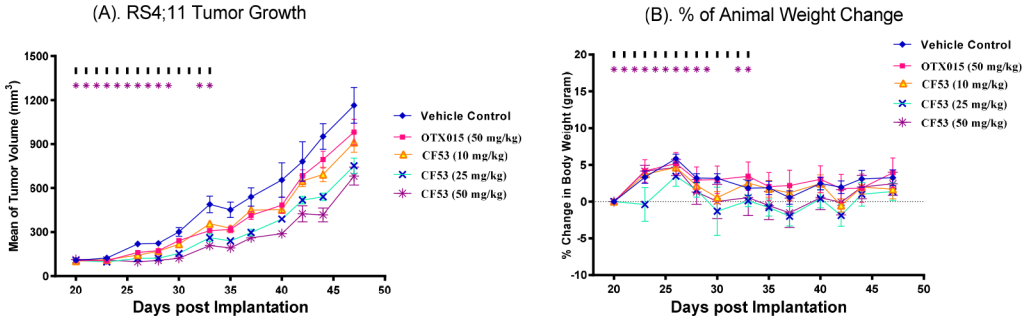

Figure 6. Antitumor efficacy study of **28** (CF53) and **3** (OTX015) in the RS4;11 xenograft model in SCID mice. These compounds were administered via oral gavage at indicated doses. (A) Tumor growth inhibition. (B) Animal weight change.

indazole or 5-aminopyrazole (S2), as shown in Scheme 1. Generally, the amine (S2) and the key intermediate (S13)

Scheme 1. Synthesis of Final Compounds[a]

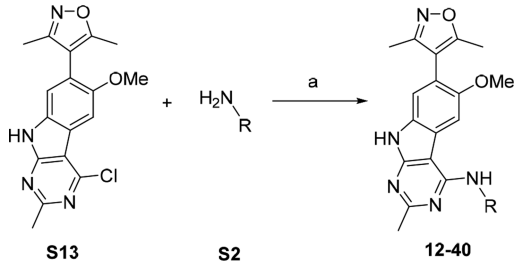

[a]Reaction conditions: (a) HCl in *i*-PrOH, reflux, or $Pd_2(dba)_3$, bis(diphenylphosphino)-1,1′-binaphthyl, base, and solvent.

were mixed in solvents, and this was followed by addition of acid or Pd catalyst. The reaction mixtures were heated and the crude products were further purified by flash chromatography, reverse-phase high-performance liquid chromatography (HPLC), or both to yield the final products.

CONCLUSIONS

We have designed and synthesized a series of 9H-pyrimido-[4,5-*b*]indole-containing compounds by elimination of the restricted rotation around a C−C bond of **9**, which yielded achiral, highly potent, and orally bioavailable BET inhibitors. Among them, compound **28** (CF53) binds to BET proteins with K_d values of 0.4−2.2 nM and shows low nanomolar potencies in cell growth inhibition of the MDA-MB-231 triple-negative breast cell line and the MOLM-13 acute leukemia cell line. It achieves excellent oral pharmacokinetics in mice, and effectively inhibits tumor growth in xenograft models in mice. Determination of the co-crystal structure of **28** with BRD4 BD1 provides a structural basis for its high binding affinity to BET proteins. Testing its binding affinities against other bromodomain-containing proteins shows that **28** is also a highly selective BET inhibitor against bromodomains. Our data show that **28** (CF53) is a potent, selective, and orally active BET inhibitor suitable for preclinical development.

EXPERIMENTAL SECTION

1. General Methods. All reactions were conducted in a round-bottomed flask equipped with a Teflon-coated magnet stirring bar. Experiments involving moisture- or air-sensitive components or both were performed under an N_2 atmosphere. Commercial reagents and anhydrous solvents were used without further purification. The crude reaction products were purified by flash column chromatography using silica gel. Further purification was performed with preparative HPLC (Waters 2545) with a C18 reverse-phase column. The mobile phase used here was a gradient flow of solvent A (water, 0.1% of TFA) and solvent B (CH_3CN, 0.1% of TFA) at a flow rate of 40 mL/min. Proton nuclear magnetic resonance (^{1}H NMR) and carbon nuclear magnetic resonance (^{13}C NMR) spectroscopy were performed in Bruker Advance 300/400 NMR spectrometers. Low-resolution ESI mass spectrum analysis was performed on a Thermo-Scientific LCQ Fleet mass spectrometer or Advion Expression mass spectrometer. The analytical UPLC model was Waters Acquity H class (UV detection at 230 and 254 nm), and the reverse-phase column used was the Acquity UPLC BEH (C18−1.7 μm, 2.1mm × 50 mm). Unless otherwise stated, all final compounds were purified to ≥95% purity, as determined by analytical UPLC analysis.

2. Synthesis of Final Compounds. *7-(3,5-Dimethylisoxazol-4-yl)-6-methoxy-2-methyl-N-(1-methyl-1H-indazol-3-yl)-9H-pyrimido[4,5-b]indol-4-amine (**12**) Method A.* S13 (90 mg) and 1-methyl-1H-indazol-3-amine (90 mg) were placed in a round-bottomed flask followed by the addition of *i*-PrOH (30 mL). A total of four drops of concentrated HCl was added via a glass pipet. The mixture was heated overnight at reflux temperature. The reaction was then concentrated on a rotary evaporator and the residue was purified by HPLC to yield 60 mg of the desired product (**12**) as the trifluoroacetate. ^{1}H NMR (300 MHz, MeOD-d4): 8.44 (d, J = 7.88 Hz, 1H), 7.84 (s, 1H), 7.68 (d, J = 8.62 Hz, 1H), 7.57 (t, J = 7.63 Hz, 1H), 7.47 (s, 1H), 7.30 (t, J = 7.55 Hz, 1H), 4.16 (s, 3H), 3.86 (s, 3H), 2.73 (s, 3H), 2.33 (s, 3H), 2.16 (s, 3H). ESI-MS: $[M + H]^+$ calcd for $C_{25}H_{24}N_7O_2$, 454.20; found, 454.42.

*7-(3,5-Dimethylisoxazol-4-yl)-6-methoxy-2-methyl-N-(1-methyl-1H-pyrazolo[3,4-b]pyridin-3-yl)-9H-pyrimido[4,5-b]indol-4-amine (**13**) Method B.* $Pd_2(dba)_3$ (18 mg, 0.02 mmol) and BINAP (26 mg, 0.04 mmol) were mixed in anhydrous toluene (5 mL), and the mixture was heated at reflux for 3−4 min. This mixture was transferred into a round-bottomed flask containing S13 (68 mg, 0.2 mmol), 1-methyl-1H-pyrazolo[3,4-*b*]pyridin-3-amine (60 mg, 0.4 mmol), K_3PO_4 (127 mg, 0.6 mmol), and toluene (15 mL). The mixture was heated at reflux overnight before being quenched with MeOH. The reaction mixture was filtered, and the filtrate was concentrated and purified by HPLC to yield 32 mg of the desired product (**13**) as the trifluoroacetate. ^{1}H NMR (300 MHz, MeOD-d4): 8.65 (d, J = 3.99 Hz, 1H), 8.38 (d, J = 8.15 Hz, 1H), 7.89, 7.48, 7.31 (dd, J = 8.08, 4.55 Hz, 1H), 4.17 (s, 3H), 3.86 (s, 3H), 2.71 (s, 3H), 2.32 (s, 3H), 2.15 (s, 3H). ESI-MS: $[M + H]^+$ calcd for $C_{24}H_{23}N_8O$, 455.19; found, 455.50.

*7-(3,5-Dimethylisoxazol-4-yl)-6-methoxy-2-methyl-N-(1-methyl-1H-pyrazolo[4,3-c]pyridin-3-yl)-9H-pyrimido[4,5-b]indol-4-amine (**14**) Method B.* S13 (70 mg) and 1-methyl-1H-pyrazolo[4,3-*c*]pyridin-3-amine (60 mg) were the substrates, and, upon HPLC purification, 47 mg of the desired product (**14**) was isolated as the trifluoroacetate.^{1}H NMR (300 MHz, $CDCl_3$): 9.71 (s, 1H), 8.46 (d, J = 6.97 Hz, 1H), 8.12 (s, 1H), 8.08 (d, J = 7.00 HZ, 1H), 7.38 (s, 1H), 4.23 (s, 3H), 3.98 (s, 3H), 2.65 (s, 3H), 2.34 (s, 3H), 2.18 (s, 3H).

*7-(3,5-Dimethylisoxazol-4-yl)-6-methoxy-2-methyl-N-(1-methyl-1H-pyrazolo[4,3-b]pyridin-3-yl)-9H-pyrimido[4,5-b]indol-4-amine (**15**, 94% Purity by UPLC Analysis) Method B.* S13 (102 mg, 0.3

DOI: 10.1021/acs.jmedchem.8b00483
J. Med. Chem. XXXX, XXX, XXX−XXX

mmol) and 1-methyl-1H-pyrazolo[4,3-*b*]pyridin-3-amine (90 mg, 0.6 mmol) were the substrates and upon HPLC purification, 27.9 mg of the desired product (**15**) was produced as the trifluoroacetate (94% purity by HPLC).^{1}H NMR (300 MHz, MeOD-d4): 8.69 (d, *J* = 3.63 Hz, 1H), 8.32 (dd, *J* = 8.69, 0.79 Hz, 1H), 8.26 (s, 1H), 7.67 (dd, *J* = 8.74, 4.41 Hz, 1H), 7.49 (s, 1H), 4.22 (s, 3H), 4.01 (s, 3H), 2.84 (s, 3H), 2.35 (s, 3H), 2.18 (s, 3H). ESI-MS: $[M + H]^+$ calcd for $C_{24}H_{23}N_8O_2$, 455.19; found, 455.42.

*N-(5-Chloro-1-methyl-1H-indazol-3-yl)-7-(3,5-dimethylisoxazol-4-yl)-6-methoxy-2-methyl-9H-pyrimido[4,5-b]indol-4-amine (**16**) Method A.* S13 (70 mg) and 5-chloro-1-methyl-1H-indazol-3-amine (100 mg) were the substrates, and, upon HPLC purification, 18 mg of the desired product (**16**) was isolated as the trifluoroacetate. ^{1}H NMR (300 MHz, MeOD-d4): 7.92 (s, 2H), 7.69 (d, *J* = 9.01 Hz, 1H), 7.52 (d, *J* = 9.01 Hz, 1H), 7.48 (s, 1H), 4.15 (s, 3H), 3.89 (s, 3H), 2.71 (s, 3H), 2.34 (s, 3H), 2.16 (s, 3H). ESI-MS: $[M + H]^+$ calcd for $C_{25}H_{23}{}^{35}ClN_7O_2$, 4808.16; found, 488.29.

*7-(3,5-Dimethylisoxazol-4-yl)-6-methoxy-N-(6-methoxy-1-methyl-1H-indazol-3-yl)-2-methyl-9H-pyrimido[4,5-b]indol-4-amine (**17**) Method A.* S13 (68 mg) and 1-methyl-6-methoxy-1H-indazol-3-amine (80 mg) were the substrates, and, upon HPLC purification, 24 mg of the desired product (**17**) was isolated as thetrifluoroacetate. ^{1}H NMR (300 MHz, MeOD-d4): 7.89 (s, 1H), 7.75 (d, *J* = 8.92 Hz, 1H), 7.47 (s, 1H), 7.07 (d, *J* = 1.95 Hz, 1H), 6.92 (dd, *J* = 8.86, 2.13 Hz, 1H), 4.11 (s, 3H), 3.95 (s, 3H), 3.90 (s, 3H), 2.77 (s, 3H), 2.33 (s, 3H), 2.16 (s, 3H). ESI-MS: $[M + H]^+$ calcd for $C_{26}H_{26}N_7O_3$, 484.21; found, 484.37.

*7-(3,5-Dimethylisoxazol-4-yl)-N-(5-fluoro-1-methyl-1H-indazol-3-yl)-6-methoxy-2-methyl-9H-pyrimido[4,5-b]indol-4-amine (**18**) Method A.* 5-Fluoro-1-methyl-1H-indazol-3-ylamine (100 mg, 0.6 mol) and S13 (102 mg, 0.3 mmol) were the substrates, and, upon HPLC purification, 17 mg of the desired product (**18**) was isolated as the trifluoroacetate. ^{1}H NMR (300 MHz, MeOD-d4): 7.93 (s, 1H), 7.71 (dd, *J* = 9.05, 3.80 Hz, 1H), 7.56 (dd, *J* = 8.80, 2.24 Hz, 1H), 7.48 (s, 1H), 7.44−7.32 (m, 1H), 4.16 (s, 3H), 3.89 (s, 3H), 2.71 (s, 3H), 2.33 (s, 3H), 2.16 (s, 3H). ESI-MS: $[M + H]^+$ calcd for $C_{25}H_{23}FN_7O_2$, 472.19; found, 472.42.

*7-(3,5-Dimethylisoxazol-4-yl)-N-(6-fluoro-1-methyl-1H-indazol-3-yl)-6-methoxy-2-methyl-9H-pyrimido[4,5-b]indol-4-amine (**19**) Method A.* 6-Fluoro-1-methyl-1H-indazol-3-ylamine (100 mg, 0.6 mol) and S13 (102 mg, 0.3 mmol) were the substrates, and, upon HPLC purification, 77 mg of the desired product (**19**) was isolated as the trifluoroacetate.^{1}HNMR (300 MHz, MeOD-d4): 8.06 (s, 1H), 7.66 (t, *J* = 7.97 Hz, 1H), 7.49 (s, 1H), 7.16−7.00 (m, 2H), 3.94 (s, 3H), 3.49 (s, 3H), 2.76 (s, 3H), 2.32 (s, 3H), 2.14 (s, 3H). ESI-MS: $[M + H]^+$ calcd for $C_{25}H_{23}FN_7O_2$, 472.19; found, 472.36.

*7-(3,5-Dimethylisoxazol-4-yl)-N-(7-fluoro-1-methyl-1H-indazol-3-yl)-6-methoxy-2-methyl-9H-pyrimido[4,5-b]indol-4-amine (**20**) Method A.* 7-Fluoro-1-methyl-1H-indazol-3-ylamine (100 mg, 0.6 mol) and S13 (102 mg, 0.3 mmol) were the substrates, and, upon HPLC purification, 50 mg of the desired product (**20**)was isolated as the trifluoroacetate. ^{1}H NMR (300 MHz, MeOD-d4): 7.83 (s, 1H), 7.63 (d, *J* = 7.94 Hz, 1H), 7.48 (s, 1H), 7.30−7.12 (m, 2H), 4.27 (s, 3H), 3.86 (s, 3H), 2.69 (s, 3H), 2.33 (s, 3H), 2.15 (s, 3H). ESI-MS: $[M + H]^+$ calcd for $C_{25}H_{23}FN_7O_2$, 472.19; found, 472.36.

*7-(3,5-Dimethylisoxazol-4-yl)-N-(4-fluoro-1-methyl-1H-indazol-3-yl)-6-methoxy-2-methyl-9H-pyrimido[4,5-b]indol-4-amine (**21**) Method A.* 4-Fluoro-1-methyl-1H-indazol-3-ylamine (102 mg, 0.6 mol) and S13 (102 mg, 0.3 mmol) were the substrates, and, upon HPLC purification, 75 mg of the desired product (**21**) was isolated as the trifluoroacetate. ^{1}H NMR (300 MHz, MeOD-d4): 7.82 (s, 1H), 7.54−7.45 (m, 2H), 7.49 (s, 1H), 6.98−6.87 (m, 1H), 4.16 (s, 3H), 3.87 (s, 3H), 2.72 (s, 3H), 2.33 (s, 3H), 2.15 (s, 3H). ESI-MS: $[M + H]^+$ calcd for $C_{25}H_{23}FN_7O_2$, 472.19; found, 472.33

*7-(3,5-Dimethylisoxazol-4-yl)-N-(1H-indazol-3-yl)-6-methoxy-2-methyl-9H-pyrimido[4,5-b]indol-4-amine (**22**) Method A.* 1H-indazol-3-ylamine (84 mg, 0.6 mol) and S13 (102 mg, 0.3 mmol) were the substrates, and, upon HPLC purification, 27 mg of the desired product (**22**) was isolated as the trifluoroacetate. ^{1}H NMR (300 MHz, MeOD-d4): 7.92 (d, *J* = 8.29 Hz, 1H), 7.74 (s, 1H), 7.64 (d, J= 8.55 Hz, 1H), 7.57−7.50 (m, 1H), 7.47 (s, 1H), 7.32−7.25 (m, 1H), 3.84 (s, 3H), 2.76 (s, 3H), 2.32 (s, 3H), 2.15 (s, 3H). ESI-MS: $[M + H]^+$, calcd for $C_{24}H_{22}N_7O_2$, 440.18; found, 440.33.

*2-(3-((7-(3,5-Dimethylisoxazol-4-yl)-6-methoxy-2-methyl-9H-pyrimido[4,5-b]indol-4-yl)amino)-1H-indazol-1-yl)ethanol (**23**) Method A.* 2-(3-Amino-1H-indazol-1-yl) ethanol (290 mg, 1.6 mol) and S13 (170 mg, 0.5 mmol) were the substrates, and, upon HPLC purification, 107 mg of the desired product (**23**) was isolated as the trifluoroacetate. ^{1}H NMR (300 MHz, MeOD-d4): 7.91 (d, *J* = 8.25 Hz, 1H), 7.84 (s, 1H), 7.70 (d, *J* = 8.65 Hz, 1H), 7.54 (t, *J* = 7.58 Hz, 1H), 7.47 (s, 1H), 7.27 (t, *J* = 7.50 Hz, 1H), 4.57 (t, *J* = 5.10 Hz, 2H), 4.05 (t, *J* = 5.10 Hz, 2H), 3.83 (s, 3H), 2.71 (s, 3H), 2.32 (s, 3H), 2.15 (s, 3H). ESI-MS: $[M + H]^+$ calcd for $C_{26}H_{26}N_7O_3$, 484.21; found, 484.25.

*N-(1,3-dimethyl-1H-pyrazol-5-yl)-7-(3,5-dimethylisoxazol-4-yl)-6-methoxy-2-methyl-9H-pyrimido[4,5-b]indol-4-amine (**24**) Method B.* S13 (68 mg) and 1,3-dimethyl-1H-pyrazol-5-amine (50 mg) were the substrates, and, upon HPLC purification, 40 mg of the desired product (**24**) was isolated as the trifluoroacetate. ^{1}H NMR (300 MHz, MeOD-d4): 7.46 (s, 1H), 7.43 (s, 1H), 6.25 (s, 1H), 3.87 (s, 3H), 3.76 (s, 3H), 2.70 (s, 3H), 2.31 (s, 3H), 2.30 (s, 3H), 2.14 (s, 3H). ESI-MS: $[M + H]^+$ calcd for $C_{22}H_{24}N_7O_2$, 418.20; found, 418.92.

*7-(3,5-Dimethylisoxazol-4-yl)-6-methoxy-2-methyl-N-(1-methyl-3-(trifluoromethyl)-1H-pyrazol-5-yl)-9H-pyrimido[4,5-b]indol-4-amine (**25**) Method B.* S13 (102 mg) and 2-methyl-5-(trifluoromethyl)pyrazol-3-amine (100 mg) were the substrates, and, upon HPLC purification, 29 mg of the desired product (**25**)was isolated as the trifluoroacetate. ^{1}H NMR (300 MHz, MeOD-d4): 7.83 (s, 1H), 7.47 (s, 1H), 6.72 (s, 1H), 3.92 (s, 3H), 3.88 (s, 3H), 2.67 (s, 3H), 2.32 (s, 3H), 2.15 (s, 3H). ESI-MS: $[M + H]^+$ calcd for $C_{22}H_{21}F_3N_7O_2$, 472.17; found, 472.33.

*7-(3,5-Dimethylisoxazol-4-yl)-N-(3-isopropyl-1-methyl-1H-pyrazol-5-yl)-6-methoxy-2-methyl-9H-pyrimido[4,5-b]indol-4-amine (**26**) Method B.* S13 (102 mg, 0.3 mmol) and 3-isopropyl-1-methyl-1H-pyrazol-5-amine (84 mg, 0.6 mmol) were the substrates, and, upon HPLC purification, 49 mg of the desired product (**26**) was isolated as the trifluoroacetate. ^{1}H NMR (300 MHz, MeOD-d4): 7.46 (s, 1H), 7.42 (s, 1H), 6.25 (s, 1H), 3.87 (s, 3H), 3.81 (s, 3H), 2.97 (septet, *J* = 6.92 Hz, 1H), 2.71 (s, 3H), 2.31 (s, 3H), 2.13 (s, 3H), 1.28 (d, *J* = 6.95 Hz, 6H). ESI-MS: $[M + H]^+$ calcd for $C_{24}H_{28}N_7O_2$, 446.23; found, 446.42.

*N-(3-tert-Butyl-1-methyl-1H-pyrazol-5-yl)-7-(3,5-dimethylisoxazol-4-yl)-6-methoxy-2-methyl-9H-pyrimido[4,5-b]indol-4-amine (**27**) Method B.* S13 (102 mg, 0.3 mmol) and 3-*tert*-butyl-1-methyl-1H-pyrazol-5-amine (100 mg, 0.6 mmol) were the substrates, and, upon HPLC purification, 49 mg of the desired product (**27**) was isolated as the trifluoroacetate. ^{1}H NMR (300 MHz, MeOD-d4): 7.45 (s, 1H), 6.26 (s, 1H), 3.88 (s, 3H), 3.82 (s, 3H), 2.71 (s, 3H), 2.31 (s, 3H), 2.14 (s, 3H), 1.32 (s, 9H). ESI-MS: $[M + H]^+$ calcd for $C_{25}H_{30}N_7O_2$, 460.25; found, 460.33.

*N-(3-Cyclopropyl-1-methyl-1H-pyrazol-5-yl)-7-(3,5-dimethylisoxazol-4-yl)-6-methoxy-2-methyl-9H-pyrimido[4,5-b]indol-4-amine (**28**) Method B.* S13 (102 mg, 0.3 mmol) and 3-cyclopropyl-1-methyl-1H-pyrazol-5-amine (90 mg, 0.6 mmol) were the substrates, and, upon HPLC purification, 53 mg of the desired product (**28**) was isolated as the trifluoroacetate. ^{1}H NMR (300 MHz, MeOD-d4): 7.45 (s, 1H), 7.25 (s, 1H), 6.09 (s, 1H), 3.86 (s, 3H), 3.75 (s, 3H), 2.71 (s, 3H), 2.31 (s, 3H), 2.14 (s, 3H), 2.00−1.80 (m, 1H), 1.00−0.90 (m, 2H), 0.76−0.68 (m, 2H). ^{13}C (NMR, 100 MHz): 165.96, 160.91, 159.64, 154.66, 154.53, 153.05, 152.73, 137.03, 131.42, 119.83, 117.44, 114.51, 113.80, 104.65, 99.54, 95.43, 56.56, 35.77, 24.51, 11.73, 10.79, 9.86, 8.11. ESI-MS: $[M + H]^+$ calcd for $C_{24}H_{26}N_7O_2$, 444.21; found, 444.33.

*N-(3-Cyclobutyl-1-methyl-1H-pyrazol-5-yl)-7-(3,5-dimethylisoxazol-4-yl)-6-methoxy-2-methyl-9H-pyrimido[4,5-b]indol-4-amine (**29**) Method B.* S13 (102 mg, 0.3 mmol) and 1-methyl-3-cyclobutyl-1H-pyrazol-5-amine (90 mg, 0.6 mmol) were the substrates, and, upon HPLC purification, 49 mg of the desired product (**29**) was isolated as the trifluoroacetate. ^{1}H NMR (300 MHz, MeOD-D4): 7.45 (s, 1H), 7.34 (s, 1H), 6.31 (s, 1H), 3.85 (s, 3H), 3.78 (s, 3H), 3.65−3.50 (m, 1H), 2.71 (s, 3H), 2.50−2.30 (m, 2H), 2.31 (s, 3H),

DOI: 10.1021/acs.jmedchem.8b00483
J. Med. Chem. XXXX, XXX, XXX−XXX

2.30−2.15 (m, 2H), 2.15−2.00 (m, 1H), 2.14 (s, 3H), 2.00−1.80 (m, 1H). ESI-MS: $[M + H]^+$ calcd for $C_{25}H_{28}N_7O_2$, 458.23; found, 458.50.

*7-(3,5-Dimethylisoxazol-4-yl)-6-methoxy-2-methyl-N-(1-methyl-3-(1,1,1-trifluoro-2-methylpropan-2-yl)-1H-pyrazol-5-yl)-9H-pyrimido[4,5-b]indol-4-amine (**30**) Method C.* $Pd_2(dba)_3$ (27 mg, 0.03 mmol) and BINAP (37 mg, 0.06 mmol) were mixed in anhydrous toluene (5 mL), and the mixture was heated at reflux for 3−4 min. This mixture was transferred into a round-bottomed flask containing S13 (102 mg, 0.3 mmol), 1-methyl-3-(1,1,1-trifluoro-2-methylpropan-2-yl)-1H-pyrazol-5-amine (120 mg, 0.6 mmol), *t*-BuONa (200 mg, 1.2 mmol), and toluene (15 mL). The mixture was heated at reflux overnight before quenching with MeOH. The reaction mixture was filtered, and the mother liquid was concentrated and purified by HPLC to yield 48 mg of **30** as the trifluoroacetate. ^1H NMR (300 MHz, MeOD-D4): 7.67 (s, 1H), 7.46 (s, 1H), 6.41 (s, 1H), 3.90 (s, 1H), 3.83 (s, 3H), 2.69 (s, 3H), 2.32 (s, 3H), 2.15 (s, 3H), 1.55 (s, 6H). ESI-MS: $[M + H]^+$ calcd for $C_{25}H_{27}F_3N_7O_2$, 514.22; found, 514.33.

*7-(3,5-Dimethylisoxazol-4-yl)-N-(1-ethyl-3-methyl-1H-pyrazol-5-yl)-6-methoxy-2-methyl-9H-pyrimido[4,5-b]indol-4-amine (**31**) Method B.* S13 (102 mg, 0.3 mmol) and 1-ethyl-3-methyl-1H-pyrazol-5-amine (75 mg, 0.6 mmol) were the substrates, and, upon HPLC purification, 19 mg of the desired product (**31**) was isolated as the trifluoroacetate. ^1H NMR (300 MHz, MeOD-d4): 7.45 (s, 1H), 7.28 (s, 1H), 6.21 (s, 1H), 4.11 (q, J = 7.22 Hz, 2H), 3.85 (s, 3H), 2.70 (s, 3H), 2.31 (s, 6H), 2.13 (s, 3H), 1.44 (t, J = 7.23 Hz, 3H). ESI-MS: $[M + H]^+$ calcd for $C_{23}H_{26}N_7O_2$, 432.21; found, 432.92.

*7-(3,5-Dimethylisoxazol-4-yl)-N-(1-isopropyl-3-methyl-1H-pyrazol-5-yl)-6-methoxy-2-methyl-9H-pyrimido[4,5-b]indol-4-amine (**32**) Method B.* S13 (70 mg) and 1-isopropyl-3-methyl-1H-pyrazol-5-amine (640 mg) were the substrates, and, upon HPLC purification, 26 mg of the desired product (**32**) was isolated as the trifluoroacetate. ^1H NMR (300 MHz, MeOD-d4): 7.45 (s, 1H), 7.18 (s, 1H), 6.18 (s, 1H), 4.59 (septet, J = 6.68 Hz, 1H), 3.83 (s, 3H), 2.70 (s, 3H), 2.32 (s, 3H), 2.30 (s, 3H), 2.13 (s, 3H), 1.47 (d, J = 6.66 Hz, 6H). ESI-MS: $[M + H]^+$ calcd for $C_{24}H_{28}N_7O_2$, 446.23; found, 446.67.

*N-(1-(tert-Butyl)-3-methyl-1H-pyrazol-5-yl)-7-(3,5-dimethylisoxazol-4-yl)-6-methoxy-2-methyl-9H-pyrimido[4,5-b]indol-4-amine (**33**). Method B.* S13 (60 mg) and 1-(*tert*-butyl)-3-methyl-1H-pyrazol-5-amine (84 mg) were the substrates, and, upon HPLC purification, 15 mg of the desired product (**33**) was isolated as the trifluoroacetate. ^1H NMR (300 MHz, MeOD-d4) δ 7.44 (s, 1H), 6.59 (s, 1H), 6.24 (s, 1H), 3.80 (s, 3H), 2.74 (s, 3H), 2.31 (s, 3H), 2.30 (s, 3H), 2.14 (s, 3H), 1.72 (s, 9H). ESI-MS: $[M + H]^+$ calcd for $C_{25}H_{30}N_7O_2$, 460.24; found, 460.55.

*N-(1-Cyclobutyl-3-methyl-1H-pyrazol-5-yl)-7-(3,5-dimethylisoxazol-4-yl)-6-methoxy-2-methyl-9H-pyrimido[4,5-b]indol-4-amine (**34**) Method B.* S13 (102 mg, 0.3 mmol) and 1-cyclobutyl-3-methyl-1H-pyrazol-5-amine (100 mg, 0.6 mmol) were the substrates, and, upon HPLC purification, 58 mg of the desired product (**34**) was isolated as the trifluoroacetate. ^1H NMR (300 MHz, MeOD-d4): 7.45 (s, 1H), 7.22 (s, 1H), 6.20 (s, 1H), 4.90−4.70 (m, 1H), 3.84 (s, 3H), 2.70−2.50 (m, 2H), 2.69 (s, 3H), 2.40−2.20 (m, 2H), 2.34 (s, 3H), 2.31 (s, 3H), 2.13 (s, 3H), 1.90−1.60 (m, 2H). ESI-MS: $[M + H]^+$ calcd for $C_{25}H_{28}N_7O_2$, 458.23; found, 548.58.

*N-(1-Cyclopentyl-3-methyl-1H-pyrazol-5-yl)-7-(3,5-dimethylisoxazol-4-yl)-6-methoxy-2-methyl-9H-pyrimido[4,5-b]indol-4-amine (**35**) Method B.* S13 (102 mg, 0.3 mmol) and 1-cyclopentyl-3-methyl-1H-pyrazol-5-amine (100 mg, 0.6 mmol) were the substrates, and, upon HPLC purification, 60 mg of the desired product (**35**)was isolated as the trifluoroacetate. ^1H NMR (300 MHz, MeOD-d4): 7.44 (s, 1H), 7.19 (s, 1H), 6.18 (s, 1H), 4.69 (quintet, J = 7.95 Hz, 1H), 3.83 (s, 3H), 2.70 (s, 3H), 2.31 (s, 3H), 2.13 (s, 3H), 2.10−2.00 (m, 4H), 2.00−1.80 (m, 2H), 1.70−1.50 (m, 2H). ESI-MS: $[M + H]^+$ calcd for $C_{26}H_{30}N_7O_2$, 472.25; found, 472.42.

*N-(1,5-Dimethyl-1H-pyrazol-3-yl)-7-(3,5-dimethylisoxazol-4-yl)-6-methoxy-2-methyl-9H-pyrimido[4,5-b]indol-4-amine (**36**) Method B.* S13 (102 mg, 0.3 mmol) and 1,5-dimethyl-1H-pyrazol-3-amine (70 mg, 0.6 mmol) were the substrates, and, upon HPLC purification, 31 mg of the desired product (**36**) was isolated as the trifluoroacetate. ^1H NMR (300 MHz, MeOD-d4): 8.24 (s, 1H), 7.46 (s, 1H), 6.25 (s, 1H), 3.98 (s, 3H), 3.90 (s, 3H), 2.84 (s, 3H), 2.39 (s, 3H), 2.33 (s, 3H), 2.16 (s, 3H). ESI-MS: $[M + H]^+$ calcd for $C_{22}H_{24}N_7O_2$, 418.20; found, 418.50.

*N-(3-Cyclopropyl-1,4-dimethyl-1H-pyrazol-5-yl)-7-(3,5-dimethylisoxazol-4-yl)-6-methoxy-2-methyl-9H-pyrimido[4,5-b]indol-4-amine (**37**) Method C.* S13 (136 mg) and 3-cyclopropyl-1,4-dimethyl-1H-pyrazol-5-amine (120 mg) were the substrates, and, upon HPLC purification, 16 mg of the desired product (**37**) was obtained as the trifluoroacetate. ^1H NMR (300 MHz, MeOD-D4): 7.45 (s, 1H), 7.30−7.00 (br, 1H), 3.84 (s, 3H), 3.72 (s, 3H), 2.71 (s, 3H), 2.31 (s, 3H), 2.13 (s, 3H), 1.94 (s, 3H), 2.00−1.80 (m, 2H), 1.00−0.75 (m, 4H). ESI-MS: $[M + H]^+$ calcd for $C_{25}H_{28}N_7O_2$, 458.23; found, 458.50.

*7-(3,5-Dimethylisoxazol-4-yl)-6-methoxy-2-methyl-N-(2-methyl-2,4,5,6-tetrahydrocyclopenta-[c]pyrazol-3-yl)-9H-pyrimido[4,5-b]-indol-4-amine (**38**) Method B.* S13 (102 mg, 0.3 mmol) and 2-methyl-2,4,5,6-tetrahydrocyclopenta [c]pyrazol-3-amine (90 mg, 0.6 mmol) were the substrates, and, upon HPLC purification, 38 mg of the desired product (**38**) was isolated as the trifluoroacetate. ^1H NMR (300 MHz, MeOD-d4): 7.46 (s, 1H), 7.27 (s, 1H), 3.85 (s, 3H), 3.82 (s, 3H), 2.80−2.70 (m, 2H), 2.73 (s, 3H), 2.56−2.34 (m, 4H), 2.31 (s, 3H), 2.14 (s, 3H). ESI-MS: $[M + H]^+$ calcd for $C_{24}H_{26}N_7O_2$, 444.21; found, 444.42.

*7-(3,5-Dimethylisoxazol-4-yl)-6-methoxy-2-methyl-N-(2-methyl-4,5,6,7-tetrahydro-2H-indazol-3-yl)-9H-pyrimido[4,5-b]indol-4-amine (**39**) Method B.* S13 (136 mg, 0.4 mmol) and 2-methyl-4,5,6,7-tetrahydro-2H-indazol-3-amine (144 mg, 1.0 mmol) were the substrates, and, upon HPLC purification, 25 mg of the desired product (**39**) was isolated as the trifluoroacetate. ^1H NMR (300 MHz, MeOD-d4): 7.45 (s, 1H), 7.14 (s, 1H), 3.83 (s, 3H), 3.80 (s, 3H), 2.80−2.60 (m, 2H), 2.71 (s, 3H), 2.40−2.20 (m, 2H), 2.31 (s, 3H), 2.13 (s, 3H), 1.90−1.76 (m, 2H), 1.76−1.60 (m, 2H). ESI-MS: $[M + H]^+$ calcd for $C_{25}H_{28}N_7O_2$, 458.23; found, 458.50.

*7-(3,5-Dimethylisoxazol-4-yl)-6-methoxy-2-methyl-N-(1-methyl-4,5,6,7-tetrahydro-1H-indazol-3-yl)-9H-pyrimido[4,5-b]indol-4-amine (**40**) Method B.* S13 (240 mg, 0.7 mmol) and 1-methyl-4,5,6,7-tetrahydro-1H-indazol-3-amine (220 mg, 1.4 mmol) were the substrates, and, upon HPLC purification, 100 mg of the desired product (**40**) was isolated as the trifluoroacetate. ^1H NMR (300 MHz, MeOD-d4): 7.71 (s, 1H), 7.45 (s, 1H), 3.90 (s, 3H), 3.81 (s, 3H), 2.77 (s, 3H), 2.71 (t, J = 6.06 Hz, 2H), 2.53 (t, J = 5.95 Hz, 2H), 2.32 (s, 3H), 2.15 (s, 3H), 1.98−1.84 (m, 2H), 1.84−1.70 (m, 2H). ESI-MS: $[M + H]^+$ calcd for $C_{25}H_{28}N_7O_2$, 458.23; found, 458.75.

3. Structure Determination of CD235. Yellow plates of CD235 were grown from a methanol−dichloromethane solution of the compound at 23 °C. A crystal of dimensions 0.17 mm × 0.07 mm × 0.02 mm was mounted on a Rigaku AFC10K Saturn 944+ CCD-based X-ray diffractometer equipped with a low-temperature device and Micromax-007HF Cu-target microfocus rotating anode (λ = 1.54187 A) operated at 1.2 kW power (40 kV, 30 mA). The X-ray intensities were measured at 85(1) K with the detector placed at a distance 42.00 mm from the crystal. A total of 2028 images were collected with an oscillation width of 1.0° in ω. The exposure times were 1 s for the low-angle images and 5 s for the high-angle ones. Rigaku d*trek images[27] were exported to CrysAlisPro[28] for processing and corrected for absorption. The integration of the data yielded a total of 16081 reflections to a maximum 2θ value of 138.75°, of which 3873 were independent and 3470 were greater than $2\sigma(I)$. The final cell constants (Table S2) were based on the *xyz* centroids of 7080 reflections above 10σ(I). Analysis of the data showed negligible decay during data collection. The structure was solved and refined with the Bruker SHELXTL (version 2016/6) software package[29] using the space group P1 bar with Z = 2 for the formula $C_{26}H_{20}N_5O_2F$. All non-hydrogen atoms were refined anisotropically with the hydrogen atoms placed in a combination of idealized and refined positions. Full matrix least-squares refinement based on F^2 converged at $R1$ = 0.0415 and $wR2$ = 0.1072 [based on $I > 2\sigma(I)$], $R1$ = 0.0458, and $wR2$ = 0.1118 for all data. Additional details are presented in Table S1 and are given as a CIF file in the Supporting Information.

DOI: 10.1021/acs.jmedchem.8b00483
J. Med. Chem. XXXX, XXX, XXX−XXX

4. Determination of Biochemical Binding Affinities to BET Proteins. Recombinant human proteins corresponding to BRD4 BD1 (residues 44−168) and BRD4 BD2 (residues 333−460) were used in the biochemical binding assays. The binding affinities of BET inhibitors to BRD4 (BD1and BD2 proteins) were determined using our established fluorescence polarization binding assays, as described previously.[23,24]

5. Determination of Co-crystal Structures for Compounds 12 and 28 Complexed with BRD4 BD1 Protein. BRD4 BD1 (residues 44−168) was cloned into a N-terminal His-TEV vector and expressed overnight at 20 °C in Rosetta cells. The BRD4 DB1 containing cells were lysed via sonication in 25 mM Tris at pH 7.5, 200 mM NaCl and 0.1% β-mercaptoethanol with protease inhibitors. The cellular debris was removed by centrifugation. The protein was purified from the soluble fraction using Ni-NTA resin (Qiagen) followed by tag cleavage with TEV protease. The cleaved protein was further purified by gel filtration on a Superdex75 column (GE Healthcare). The final buffer for BRD4 BD1 was 25 mM Tris at pH 8.5, 0.2 M NaCl, and 1 mM TCEP.

For crystallization, BRD4 BD1 was concentrated to 12.1 mg/mL then incubated with a 2-fold molar excess of compound **28** (CF53). Crystals grew from drops containing equal volumes of protein and well solution (20% PEG 3350 and 0.2 M potassium chloride). Prior to data collection, crystals were cryoprotected in well solution containing 25% ethylene glycol. For BRD4 BD2 crystallization, the protein was concentrated to 8.3 mg/mL and incubated with a 3-fold molar excess of **12** followed by a 1 h incubation with 0.5% β-mercaptoethanol at 20 °C. Crystals grew in a drop setup against 50−75% PEG 400 and 0.1 M imidazole, pH 8.0, which proved to be cryoprotective. Data were collected at the Advance Photon Source at Argonne National Lab on the LS-CAT beamlines 21-ID-D (BRD 4 BD1-CF53) and 21-ID-G (BRD4 BD2-**12**). Diffraction data were processed with HKL2000[30] and the structures solved by molecular replacement using MOLREP[31] for BRD4 BD1 with PDB code 4LYI as a starting model or Phaser[32] for BRD4 BD2 using PDB code 2OUO as a starting model. The structures were refined with Buster[33] and electron density fit with COOT.[34] The protein structures were validated using Molprobity.[35] Ligand structures and restraints were created using grade.[33] Refined ligand statistics were obtained from the PDB Validation Server. Data refinement and statistics are given in Table S2 in the Supporting Information.

6. Cell Growth Inhibition Assay. All human cancer cell lines were purchased from the American Type Culture Collection. Cells were used within 3 months after thawing and were cultured as recommended. In cell growth assay, cells were seeded in 96-well cell culture plates at 10 000 cells per well for leukemia cells and 3000 cells per well for breast cancer cells in 75 μL of culture medium. Compounds were serially diluted in culture medium, and 75 μL of the diluted compounds was added to the plates. The cells were then cultured for 4 days. Cell growth was evaluated by adehydrogenase-based WST-8 assay (Dojindo Molecular Technologies). The WST-8 reagent was added to the plate at a final concentration of 10% (v/v), incubated for 1−3 h, and read at 450 nm using a Tecan Infinite M1000 multimode microplate reader (Tecan, Morrisville, NC). The readings were normalized to the DMSO-treated cells, and the IC_{50} was calculated by nonlinear regression analysis using GraphPad Prism 6 software.

7. Pharmacokinetics Studies. All animal experiments were approved by the University of Michigan Committee on Use and Care of Animals and Unit for Laboratory Animal Medicine under the approved protocol (no. PRO00005315 with principal investigator Shaomeng Wang). Limited pharmacokinetics of compounds **26**, **27**, **28**, **33**, **38**, and **39** were determined in severe combined immunodeficient (SCID) mice bearing MDA-MB-231 tumor, and the corresponding drug was orally administrated at 50 mg/kg dose.

The full pharmacokinetics of compounds **28** were determined in Balb/c mice following intravenous (IV) dosing at 5.0 mg/kg or oral (PO) dosing at 25 mg/kg. The tested compound was dissolved in a vehicle containing 20% (v/v) PEG400, 6% (v/v) CremophorEL and 74% (v/v) phosphate-buffered saline (PBS). Blood samples (100 μL) were collected from rats with a catheter at 0, 5, 15, and 30 min and 1, 2, 4, 6, 8, and 24 h after administration of the drugs. The blood samples were centrifuged at 15 000 rpm for 10 min, and then the supernatant plasma was stored at −80 °C until analysis. Plasma concentrations of the compounds were determined by the liquid chromatography−tandem mass spectrometry (LC−MS/MS) method developed and validated for this study. The LC−MS/MS method consisted of a Shimadzu HPLC system, and chromatographic separation of tested compounds was achieved using a Waters XBridge-C18 column (5 cm × 2.1 mm, 3.5 μm). An AB SciexQTrap 4500 mass spectrometer equipped with an electrospray ionization source (Applied Biosystems, Toronto, Canada) in the positive-ion multiple reaction monitoring mode was used for detection. The mobile phases were 0.1% formic acid in purified water (A) and 0.1% formic acid in CH_3CN (B). The gradient (B) was held at 10% (0−0.3 min), increased to 95% at 0.7 min, stayed at an isocratic 95% B for 2.3 min, and then immediately stepped back down to 10% for 2 min of re-equilibration. The flow rate was set at 0.4 mL/min. All pharmacokinetic parameters were calculated by non-compartmental methods using WinNonlin, version 3.2 (Pharsight Corporation, Mountain View, CA).

8. Efficacy Studies in the RS4;11 and MDA-MB-231 Xenograft Models in Mice. All efficacy experiments were done under the guidelines of the University of Michigan Committee for Use and Care of Animals and using an approved animal protocol (no. PRO00005315, principal investigator Shaomeng Wang). To develop xenograft tumors, 5×10^6 RS4;11 or MDA-MB-231 cells with 50% Matrigel were injected subcutaneously on the dorsal side of SCID mice, obtained from Charles River (one tumor per mouse). When tumors reached ca. 100 mm^3, mice were randomly assigned to treatment and vehicle control groups. Animals were monitored daily for any signs of toxicity and weighed 2−3 times per week during the treatment and then weighed at least weekly after the treatment ended. Tumor size was measured 2−3 times per week by electronic calipers during the treatment period and at least weekly after the treatment ended. Tumor volume was calculated as $V = L \times W^2/2$, where L is the length and W is the width of the tumor. The p value was calculated using an unpaired t test (two-tailed) using GraphPad Prism 7 software.

■ ASSOCIATED CONTENT

Supporting Information

The Supporting Information is available free of charge on the ACS Publications website at DOI: 10.1021/acs.jmedchem.8b00483.

Tables showing crystal data nd structure refinement and crystallography data collection and refinement statistics. (PDF)

A molecular formula strings file with in vitro activity data (CSV)

Coordinates file for single crystal structure of compound **10** (CIF)

Accession Codes

Atomic coordinates have been deposited in the Protein Data Bank (PDB code: 6C7Q for compound **12** and 6C7R for compound **28**).

■ AUTHOR INFORMATION

Corresponding Author

*E-mail: shaomeng@umich.edu; phone: 734-615-0362; fax: 734-647-9647.

ORCID

Bing Zhou: 0000-0003-1813-8035

Shaomeng Wang: 0000-0002-8782-6950

DOI: 10.1021/acs.jmedchem.8b00483
J. Med. Chem. XXXX, XXX, XXX−XXX

Present Addresses

[⊥]Y.Z. and B.Z.: State Key Laboratory of Drug Research, Shanghai Institute of Materia Medica, Chinese Academy of Sciences, Shanghai 201203, China.

[#]X.R.: Institute for Neurodegenerative Diseases, University of California, San Francisco, CA 94143, United States.

Author Contributions

[○]Y.Z. and B.Z. contributed equally.

Notes

The authors declare the following competing financial interest(s): Multiple patents have been filed by University of Michigan on this class of BET bromodomain in inhibitors, which have been licensed by OncoFusion Therapeutics Inc. S.W., Y.Z., B.Z., L.L., L.B., C.-Y.Y., B.W., T.Z., D.S., D.M., and X.L. are inventors of the BET bromodomain inhibitors reported in this manuscript and receive royalties from University of Michigan. S.W. also owns stock in and serves as a consultant for OncoFusion Therapeutics Inc. The University of Michigan and S.W. have also received a research contract from OncoFusion Therapeutics, Inc.

■ ACKNOWLEDGMENTS

This study is supported in part by the Prostate Cancer Foundation, OncoFusion Therapeutics, Inc., the University of Michigan Prostate Cancer SPORE grant (NIH/NCI, Grant P50 CA186786) and the University of Michigan Comprehensive Cancer Core grant (NIH/NCI, Grant P30CA046592). Use of the Advanced Photon Source, an Office of Science User Facility operated for the U.S. Department of Energy (DOE) Office of Science by Argonne National Laboratory, was supported by the U.S. DOE under Contract DE-AC02-06CH11357. The Life Sciences Collaborative Access Team (LS-CAT) at Sector 21 of the Advanced Photon Source at Argonne National Laboratory was supported by the Michigan Economic Development Corporation and the Michigan Technology Tri-Corridor (Grant 085P1000817). We thank Dr. David Smith of LS-CAT for his assistance with crystal screening and remote data collection. The content is solely the responsibility of the authors and does not necessarily represent the official views of the National Institutes of Health or other funding agencies.

■ ABBREVIATIONS USED

BET, bromodomain and extra-terminal; BD1, first bromodomain starting from the N terminal; BD2, second bromodomain starting from the N terminal; BINAP, (1,1′-binaphthalene-2,2′-diyl)bis(diphenylphosphine); BRD2, bromodomain-containing protein 2; BRD3, bromodomain-containing protein 3; BRD4, bromodomain-containing protein 4; CL, volume of plasma cleared of the drug per unit time; SCID, severe combined immunodeficient; TGI, tumor growth inhibition; V_z, volume of distribution

■ REFERENCES

(1) Belkina, A. C.; Denis, G. V. BET domain co-regulators in obesity, inflammation and cancer. *Nat. Rev. Cancer* **2012**, *12*, 465−477.

(2) Filippakopoulos, P.; Knapp, S. Targeting bromodomains: epigenetic readers of lysine acetylation. *Nat. Rev. Drug Discovery* **2014**, *13*, 337−356.

(3) Smith, S. G.; Zhou, M. M. The bromodomain: A new target in emerging epigenetic medicine. *ACS Chem. Biol.* **2016**, *11*, 598−608.

(4) Shang, E.; Salazar, G.; Crowley, T. E.; Wang, X.; Lopez, R. A.; Wang, X.; Wolgemuth, D. J. Identification of unique, differentiation stage-specific patterns of expression of the bromodomain-containing genes Brd2, Brd3, Brd4, and Brdt in the mouse testis. *Gene Expression Patterns* **2004**, *4*, 513−519.

(5) Florence, B.; Faller, D. V. You BET-CHA: A novel family of transcriptional regulators. *Front. Biosci., Landmark Ed.* **2001**, *6*, D1008−D1018.

(6) Pivot-Pajot, C.; Caron, C.; Govin, J.; Vion, A.; Rousseaux, S.; Khochbin, S. Acetylation-dependent chromatin reorganization by BRDT, a testis-specific bromodomain-containing protein. *Mol. Cell. Biol.* **2003**, *23*, 5354−5365.

(7) LeRoy, G.; Rickards, B.; Flint, S. J. The double bromodomain proteins Brd2 and Brd3 couple histone acetylation to transcription. *Mol. Cell* **2008**, *30*, 51−60.

(8) Dey, A.; Chitsaz, F.; Abbasi, A.; Misteli, T.; Ozato, K. The double bromodomain protein Brd4 binds to acetylated chromatin during interphase and mitosis. *Proc. Natl. Acad. Sci. U. S. A.* **2003**, *100*, 8758−8763.

(9) Filippakopoulos, P.; Picaud, S.; Mangos, M.; Keates, T.; Lambert, J. P.; Barsyte-Lovejoy, D.; Felletar, I.; Volkmer, R.; Muller, S.; Pawson, T.; Gingras, A. C.; Arrowsmith, C. H.; Knapp, S. Histone recognition and large-scale structural analysis of the human bromodomain family. *Cell* **2012**, *149*, 214−231.

(10) Filippakopoulos, P.; Qi, J.; Picaud, S.; Shen, Y.; Smith, W. B.; Fedorov, O.; Morse, E. M.; Keates, T.; Hickman, T. T.; Felletar, I.; Philpott, M.; Munro, S.; McKeown, M. R.; Wang, Y.; Christie, A. L.; West, N.; Cameron, M. J.; Schwartz, B.; Heightman, T. D.; La Thangue, N.; French, C. A.; Wiest, O.; Kung, A. L.; Knapp, S.; Bradner, J. E. Selective inhibition of BET bromodomains. *Nature* **2010**, *468*, 1067−1073.

(11) Theodoulou, N. H.; Tomkinson, N. C. O.; Prinjha, R. K.; Humphreys, P. G. Clinical progress and pharmacology of small molecule bromodomain inhibitors. *Curr. Opin. Chem. Biol.* **2016**, *33*, 58−66.

(12) Postel-Vinay, S.; Herbschleb, K.; Massard, C.; Woodcock, V.; Ocker, M.; Wilkinson, G.; Walter, A.; Ewerton, F.; Poelman, M.; Middleton, M.; Soria, J. C. First-in-human phase I dose escalation study of the bromodomain and extra-terminal motif (BET) inhibitor BAY 1238097 in subjects with advanced malignancies. *Eur. J. Cancer* **2016**, *69*, S7−S8.

(13) Liu, Z.; Wang, P.; Chen, H.; Wold, E. A.; Tian, B.; Brasier, A. R.; Zhou, J. Drug discovery targeting bromodomain-containing protein 4. *J. Med. Chem.* **2017**, *60*, 4533−4558.

(14) Stathis, A.; Zucca, E.; Bekradda, M.; Gomez-Roca, C.; Delord, J. P.; de la Motte Rouge, T.; Uro-Coste, E.; de Braud, F.; Pelosi, G.; French, C. A. Clinical response of carcinomas harboring the BRD4-NUT oncoprotein to the targeted bromodomain inhibitor OTX015/MK-8628. *Cancer Discovery* **2016**, *6*, 492−500.

(15) Thieblemont, C.; Stathis, A.; Inghirami, G.; Karlin, L.; Morschhauser, F.; Gleeson, M.; Broussais, F.; Amorim, S.; Salles, G.; Facon, T.; Cunningham, D.; Vey, N.; Bourdel, F.; Herait, P.; Zucca, E. A phase 1 study of the BET-bromodomain inhibitor OTX015 in patients with non-leukemic hematologic malignancies. *Blood* **2014**, *124*.4417

(16) Shapiro, G. I.; Dowlati, A.; LoRusso, P. M.; Eder, J. P.; Anderson, A.; Do, K. T.; Kagey, M. H.; Sirard, C.; Bradner, J. E.; Landau, S. B. Abstract A49: Clinically efficacy of the BET bromodomain inhibitor TEN-010 in an open-label substudy with patients with documented NUT-midline carcinoma (NMC). *Mol. Cancer Ther.* **2015**, *14*, A49.

(17) Mirguet, O.; Gosmini, R.; Toum, J.; Clement, C. A.; Barnathan, M.; Brusq, J. M.; Mordaunt, J. E.; Grimes, R. M.; Crowe, M.; Pineau, O.; Ajakane, M.; Daugan, A.; Jeffrey, P.; Cutler, L.; Haynes, A. C.; Smithers, N. N.; Chung, C. W.; Bamborough, P.; Uings, I. J.; Lewis, A.; Witherington, J.; Parr, N.; Prinjha, R. K.; Nicodeme, E. Discovery of epigenetic regulator I-BET762: lead optimization to afford a clinical candidate inhibitor of the BET bromodomains. *J. Med. Chem.* **2013**, *56*, 7501−7515.

DOI: 10.1021/acs.jmedchem.8b00483
J. Med. Chem. XXXX, XXX, XXX−XXX

(18) Albrecht, B. K.; Gehling, V. S.; Hewitt, M. C.; Vaswani, R. G.; Cote, A.; Leblanc, Y.; Nasveschuk, C. G.; Bellon, S.; Bergeron, L.; Campbell, R.; Cantone, N.; Cooper, M. R.; Cummings, R. T.; Jayaram, H.; Joshi, S.; Mertz, J. A.; Neiss, A.; Normant, E.; O'Meara, M.; Pardo, E.; Poy, F.; Sandy, P.; Supko, J.; Sims, R. J., 3rd; Harmange, J. C.; Taylor, A. M.; Audia, J. E. Identification of a benzoisoxazoloazepine inhibitor (CPI-0610) of the bromodomain and extra-terminal (BET) family as a candidate for human clinical trials. *J. Med. Chem.* **2016**, *59*, 1330−1339.

(19) Bui, M. H.; Lin, X.; Albert, D. H.; Li, L.; Lam, L. T.; Faivre, E. J.; Warder, S. E.; Huang, X.; Wilcox, D.; Donawho, C. K.; Sheppard, G. S.; Wang, L.; Fidanze, S.; Pratt, J. K.; Liu, D.; Hasvold, L.; Uziel, T.; Lu, X.; Kohlhapp, F.; Fang, G.; Elmore, S. W.; Rosenberg, S. H.; McDaniel, K. F.; Kati, W. M.; Shen, Y. Preclinical characterization of BET family bromodomain inhibitor ABBV-075 suggests combination therapeutic strategies. *Cancer Res.* **2017**, *77*, 2976−2989.

(20) McDaniel, K. F.; Wang, L.; Soltwedel, T.; Fidanze, S. D.; Hasvold, L. A.; Liu, D. C.; Mantei, R. A.; Pratt, J. K.; Sheppard, G. S.; Bui, M. H.; Faivre, E. J.; Huang, X. L.; Li, L. M.; Lin, X. Y.; Wang, R. Q.; Warder, S. E.; Wilcox, D.; Albert, D. H.; Magoc, T. J.; Rajaraman, G.; Park, C. H.; Hutchins, C. W.; Shen, J. W. J.; Edalji, R. P.; Sun, C. H. C.; Martin, R.; Gao, W. Q.; Wong, S. M.; Fang, G. W.; Elmore, S. W.; Shen, Y.; Kati, W. M. Discovery of N-(4-(2,4-difluorophenoxy)-3-(6-methyl-7-oxo-6,7-dihydro-1H-pyrrolo[2,3-c]pyridin-4-yl)phenyl)-ethanesulfonamide (ABBV-075/Mivebresib), a potent and orally available bromodomain and extraterminal domain (BET) family bromodomain inhibitor. *J. Med. Chem.* **2017**, *60*, 8369−8384.

(21) Siebel, A. L.; Trinh, S. K.; Formosa, M. F.; Mundra, P. A.; Natoli, A. K.; Reddy-luthmoodoo, M.; Huynh, K.; Khan, A. A.; Carey, A. L.; van Hall, G.; Cobelli, C.; Dalla-Man, C.; Otvos, J. D.; Rye, K. A.; Johansson, J.; Gordon, A.; Wong, N. C. W.; Sviridov, D.; Barter, P.; Duffy, S. J.; Meikle, P. J.; Kingwell, B. A. Effects of the BET-inhibitor, RVX-208 on the HDL lipidome and glucose metabolism in individuals with prediabetes: A randomized controlled trial. *Metab., Clin. Exp.* **2016**, *65*, 904−914.

(22) Nicholls, S. J.; Puri, R.; Wolski, K.; Ballantyne, C. M.; Barter, P. J.; Brewer, H. B.; Kastelein, J. J. P.; Hu, B.; Uno, K.; Kataoka, Y.; Herrman, J. P. R.; Merkely, B.; Borgman, M.; Nissen, S. E. Effect of the BET protein inhibitor, RVX-208, on progression of coronary atherosclerosis: results of the phase 2b, randomized, double-Blind, multicenter, ASSURE trial. *Am. J. Cardiovasc. Drugs* **2016**, *16*, 55−65.

(23) Zhao, Y.; Bai, L.; Liu, L.; McEachern, D.; Stuckey, J. A.; Meagher, J. L.; Yang, C. Y.; Ran, X.; Zhou, B.; Hu, Y.; Li, X.; Wen, B.; Zhao, T.; Li, S.; Sun, D.; Wang, S. Structure-based discovery of 4-(6-methoxy-2-methyl-4-(quinolin-4-yl)-9H-pyrimido[4,5-b]indol-7-yl)-3,5-dimethy lisoxazole (CD161) as a potent and orally bioavailable BET bromodomain inhibitor. *J. Med. Chem.* **2017**, *60*, 3887−3901.

(24) Ran, X.; Zhao, Y.; Liu, L.; Bai, L.; Yang, C. Y.; Zhou, B.; Meagher, J. L.; Chinnaswamy, K.; Stuckey, J. A.; Wang, S. Structure-based design of gamma-carboline analogues as potent and specific BET bromodomain inhibitors. *J. Med. Chem.* **2015**, *58*, 4927−4939.

(25) Picaud, S.; Wells, C.; Felletar, I.; Brotherton, D.; Martin, S.; Savitsky, P.; Diez-Dacal, B.; Philpott, M.; Bountra, C.; Lingard, H.; Fedorov, O.; Muller, S.; Brennan, P. E.; Knapp, S.; Filippakopoulos, P. RVX-208, an inhibitor of BET transcriptional regulators with selectivity for the second bromodomain. *Proc. Natl. Acad. Sci. U. S. A.* **2013**, *110*, 19754−19759.

(26) Kruger, A. W.; Rozema, M. J.; Chu-Kung, A.; Gandarilla, J.; Haight, A. R.; Kotecki, B. J.; Richter, S. M.; Schwartz, A. M.; Wang, Z. The discovery and development of a safe, practical synthesis of ABT-869. *Org. Process Res. Dev.* **2009**, *13*, 1419−1425.

(27) Rigaku. CrystalClear Expert, version *2.0 r16*; *Rigaku Americas and Rigaku Corporation*; Rigaku: Tokyo, Japan, 2014.

(28) Rigaku. CrysAlis^{PRO} software system, version *1.171.38.41*; Rigaku Corporation, Oxford, United Kingdom; accessed 2015.

(29) Sheldrick, G. M. Crystal structure refinement with SHELXL. *Acta Crystallogr., Sect. C: Struct. Chem.* **2015**, *71*, 3−8.

(30) Otwinowski, Z.; Minor, W. Processing of X-ray diffraction data collected in oscillation mode. *Methods Enzymol.* **1997**, *276*, 307−326.

(31) Vagin, A.; Teplyakov, A. MOLREP: an automated program for molecular replacement. *J. Appl. Crystallogr.* **1997**, *30*, 1022−1025.

(32) Mccoy, A. J.; Grosse-Kunstleve, R. W.; Adams, P. D.; Winn, M. D.; Storoni, L. C.; Read, R. J. Phaser crystallographic software. *J. Appl. Crystallogr.* **2007**, *40*, 658−674.

(33) Bricogne, G. B. E.; Brandl, M.; Flensburg, C.; Keller, P.; Paciorek, W.; Roversi, P.; Sharff, A.; Smart, O. S.; Vonrhein, C.; Womack, T. O. *BUSTER version X.Y.Z.*; Global Phasing Ltd.: Cambridge, United Kingdom; 2011.

(34) Emsley, P.; Lohkamp, B.; Scott, W. G.; Cowtan, K. Features and development of Coot. *Acta Crystallogr., Sect. D: Biol. Crystallogr.* **2010**, *66*, 486−501.

(35) Chen, V. B.; Arendall, W. B.; Headd, J. J.; Keedy, D. A.; Immormino, R. M.; Kapral, G. J.; Murray, L. W.; Richardson, J. S.; Richardson, D. C. MolProbity: all-atom structure validation for macromolecular crystallography. *Acta Crystallogr., Sect. D: Biol. Crystallogr.* **2010**, *66*, 12−21.

DOI: 10.1021/acs.jmedchem.8b00483
J. Med. Chem. XXXX, XXX, XXX−XXX